DSF – 29/99
astro – ph/9907420

Primordial Nucleosynthesis: Accurate Predictions

S. Esposito, G. Mangano, G. Miele, and O. Pisanti[a]*

[a]Dipartimento di Fisica, Universitá di Napoli "Federico II", and INFN, Sezione di Napoli, Mostra D'Oltremare Pad. 20, I-80125 Napoli, Italy

Big Bang Nucleosynthesis (BBN) represents a key subject of modern cosmology since it is a powerful tool to study fundamental interactions. In the recent years, the improvement on the measurement accuracy of light primordial nuclei abundances allowed BBN to enter in a sort of *precision* era. In view of this, a great theoretical effort has been devoted to make theoretical predictions comparably accurate. Unfortunately, as far as D, ^3He and ^7Li are concerned, the theoretical uncertainty on their primordial abundances is greatly dominated by a poor knowledge of many nuclear reactions involved in their production. On the contrary, the ^4He abundance results into a robust prediction and thus an effort to reduce at less than 1% its theoretical uncertainty is meaningful.

To improve the accuracy on the prediction of ^4He abundance in Ref. [1] we performed a thoroughly analysis of all corrections to the proton/neutron conversion rates, $\nu_e + n \leftrightarrow e^- + p$, $e^+ + n \leftrightarrow \overline{\nu}_e + p$, $n \leftrightarrow e^- + \overline{\nu}_e + p$ which fix at the freeze out temperature $\sim 1\ MeV$ the neutron to proton density ratio. The Born rates, obtained in the tree level $V-A$ limit and with infinite nucleon mass, have been corrected to take into account three classes of relevant effects: electromagnetic radiative corrections, finite nucleon mass corrections and plasma effects.

*Talk given by G. Miele at the *International Workshop on Particles in Astrophysics and Cosmology: From Theory to Observation*, Valencia 1999.

1. The total corrections to Born rates

Let us consider for example, the averaged rate per nucleon for process $n \rightarrow e^- + \overline{\nu}_e + p$. In the simple $V-A$ tree level, and in the limit of infinite nucleon mass (*Born approximation*), one has

$$\omega_B = \frac{G_F^2 \left({C_V}^2 + 3{C_A}^2 \right)}{2\pi^3} \int_0^\infty d|\mathbf{p}'|\, |\mathbf{p}'|^2\, q_0^2 \times \Theta(q_0)\, \left[1 - F_\nu(q_0)\right] \left[1 - F_e(p'_0)\right] , \qquad (1)$$

$\mathbf{p}'$ and p'_0 are the electron momentum and energy, and q_0 the neutrino energy. The functions F_ν and F_e denote the neutrino (antineutrino) and electron (positron) Fermi distributions, respectively [1,2].

The accuracy of Born approximation can be tested by comparing, for example, the prediction for neutron lifetime obtained from (1) in the limit of vanishing temperature, $\tau_n \simeq 961\ s$, with the experimental value $\tau_n^{ex} = (886.7 \pm 1.9)\ s$ [3]. To recover the experimental value, a correction of about 8% is expected to come from radiative and/or finite nucleon mass effects. In Figure 1 the Born rates for $n \rightarrow p$ processes are reported. In Figure 2 the total corrections, listed above, to Born rates are shown. They are essentially dominated by radiative and *kinetic* corrections which at low temperature amount to 8% of the total rates.

2. The set of equations for BBN

The BBN equations [2] can be transformed in a set of $N_{nuc} + 1$ differential equations for

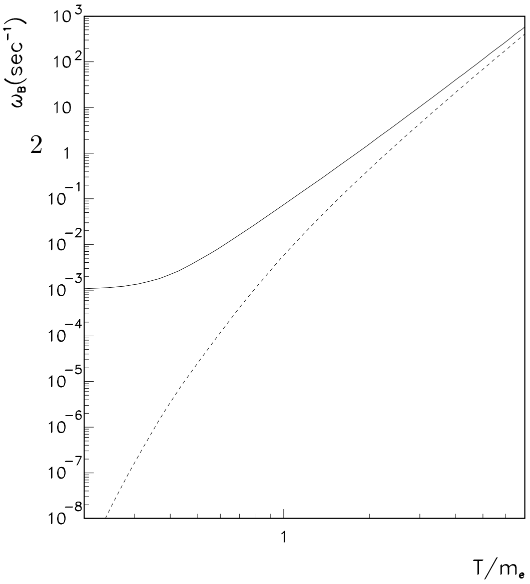

Figure 1. The total Born rates, ω_B, for $n \to p$ (solid line) and $p \to n$ transitions (dashed line).

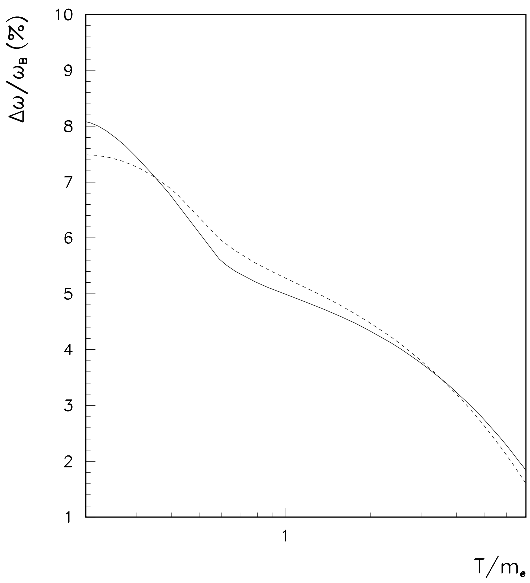

Figure 2. The total corrections to Born rates for $n \leftrightarrow p$ transitions (the same notation of Figure 1 is adopted).

$\hat{h} \equiv n_B/T^3$ and the nuclide relative abundances X_i with $z = m_e/T$ as the evolution parameter. In terms of these new variables the BBN set of equations becomes

$$\frac{d\hat{h}}{dz} = \left[1 - \widehat{H}\ G\right] \frac{3\hat{h}}{z}, \tag{2}$$

$$\frac{dX_i}{dz} = G\ \frac{\widehat{\Gamma}_i}{z} \qquad i = 1, ..., N_{nuc} \quad , \tag{3}$$

where ($\Theta = \Theta(z_D - z)$)

$$G = \left[\sum_\alpha (4\hat{\rho}_\alpha - z\frac{\partial \hat{\rho}_\alpha}{\partial z}) + 4\Theta\hat{\rho}_\nu + \frac{3}{2}\hat{h}\sum_j X_j \right] \times \left\{ 3 \left[\sum_\alpha (\hat{\rho}_\alpha + \hat{\rm p}_\alpha) + \frac{4}{3}\Theta\hat{\rho}_\nu + \hat{h}\sum_j X_j \right] \widehat{H} + \hat{h}\sum_j \left(z\Delta\widehat{M}_j + \frac{3}{2}\right) \widehat{\Gamma}_j \right\}^{-1} \tag{4}$$

In the previous equations $z_D = m_e/T_D$ (T_D is the neutrino decoupling temperature), $\alpha = e, \gamma$, and the dimensionless Hubble parameter $\widehat{H} = H/m_e$ reads

$$\widehat{H} = \sqrt{\frac{8\pi}{3}\frac{m_e}{M_P}\frac{1}{z^2}\left[\hat{\rho}_\gamma + \hat{\rho}_e + \hat{\rho}_\nu + \hat{h}\left(z\widehat{M}_u + \sum_j \left(z\Delta\widehat{M}_j + \frac{3}{2}\right) X_j \right)\right]}\ . \tag{5}$$

The quantities $\widehat{M}_u = M_u/m_e$, $\Delta\widehat{M}_j = \Delta M_j/m_e$, $\widehat{\Gamma}_j = \Gamma_j/m_e$ are the dimensionless atomic mass unit, mass excess and rate, respectively.

The initial value for (2) is provided in terms of the final baryon to photon density ratio η according to the equation

$$\hat{h}_{in} = \frac{2\zeta(3)}{\pi^2}\eta_{in} = \frac{11}{4}\ \frac{2\zeta(3)}{\pi^2}\eta \quad . \tag{6}$$

The condition of Nuclear Statistical Equilibrium (NSE), very well satisfied at the initial temperature $T_{in} = 10\ MeV$, fixes the initial nuclide relative abundances. From NSE one gets

$$X_i(T_{in}) = \frac{g_i}{2}\left(\zeta(3)\sqrt{\frac{8}{\pi}}\right)^{A_i - 1} A_i^{\frac{3}{2}}\eta^{A_i-1} \times \left(\frac{T_{in}}{M_N}\right)^{\frac{3}{2}(A_i-1)} X_p^{Z_i}\, X_n^{A_i - Z_i}\, e^{\frac{B_i}{T_{in}}}, \tag{7}$$

where B_i denotes the binding energy.

3. Light Element Abundances

By using in the BBN equations the corrected rates for $n \leftrightarrow p$ processes one can predict, with high accuracy, the primordial values for D, ${}^3He$, ${}^4He$ and ${}^7Li$

$$Y_2 = \frac{X_3}{X_2} \ , \qquad Y_3 = \frac{X_5}{X_2} \ ,$$
$$Y_4 = \frac{M_6 \ X_6}{\sum_j M_j \ X_j} \ , \qquad Y_7 = \frac{X_8}{X_2} \quad . \tag{8}$$

Using the results of [4] to quantify the uncertainties coming from nuclear reaction processes, on can observe that only for Y_4 the correction to Born rates affects result on Y_4 by an amount larger than the theoretical uncertainties, including nuclear reactions. For D, ${}^3He$ and ${}^7Li$ the uncertainty, due to the poor knowledge of nuclear reaction rates, is estimated to be of the order of $(10 \div 30)\%$ [4], thus much less than the effects of radiative/thermal correction on $n \leftrightarrow p$ rates.

In Fig. 3 the predictions on Y_4 are shown versus η for $N_\nu = 2, 3, 4$ and for a 1 σ variation of τ_n^{ex}. The two experimental estimates for the primordial ${}^4He$ mass fraction, $Y_4^{(l)} = 0.234 \pm 0.002 \pm 0.005$ and $Y_4^{(h)} = 0.243 \pm 0.003$ (see for example [5]) are the horizontal bands. Fig.s 4 and 5 show the predictions for D and ${}^7Li$ abundances. Note that, due to the negligible variation of Y_2 and Y_7 on small τ_n changes, no splitting of predictions for 1 σ variation of τ_n^{ex} is present.

4. Conclusions

A detailed study of the effects on primordial abundances of the radiative, finite nucleon mass, thermal and plasma corrections to Born rates $n \leftrightarrow p$ has been recently carried out [2]. This analysis which has reduced the uncertainty on Y_4 to less than 1% has been performed using an update version of the BBN standard code [6].

REFERENCES

1. S. Esposito, G. Mangano, G. Miele, and O. Pisanti, *Nucl. Phys.* **B540** (1999) 3.
2. S. Esposito, G. Mangano, G. Miele, and O. Pisanti, astro-ph/9906232.
3. C. Caso *et al.*, *Eur. Phys. Jour.* **C3** (1998) 1.
4. G. Fiorentini, E. Lisi, S. Sarkar, and F.L. Villante, *Phys. Rev.* **D58** (1998) 063506.
5. S. Sarkar, astro-ph/9903183.

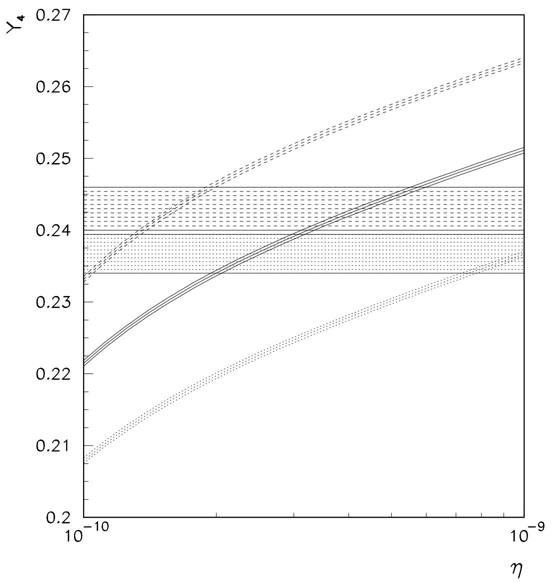

Figure 3. The ${}^4He$ mass fraction, Y_4, versus η. The three solid lines are, from larger to lower values of Y_4, the predictions corresponding to $N_\nu = 3$ and $\tau_n^{ex} = 888.6$ s, 886.7 s, 884.8 s, respectively. Analogously, the dashed lines correspond to $N_\nu = 4$ and the dotted ones to $N_\nu = 2$. The dotted and dashed horizontal band are the experimental values $Y_4^{(l)}$ and $Y_4^{(h)}$

6. R.V. Wagoner, W.A. Fowler, and F. Hoyle, *Astrophys. J.* **148** (1967) 3; R.V. Wagoner, *Astrophys. J. Suppl.* **18** (1969) 247; R.V. Wagoner, *Astrophys. J.* **179** (1973) 343; L. Kawano, preprint FERMILAB-Pub-88/34-A; preprint FERMILAB-Pub-92/04-A.

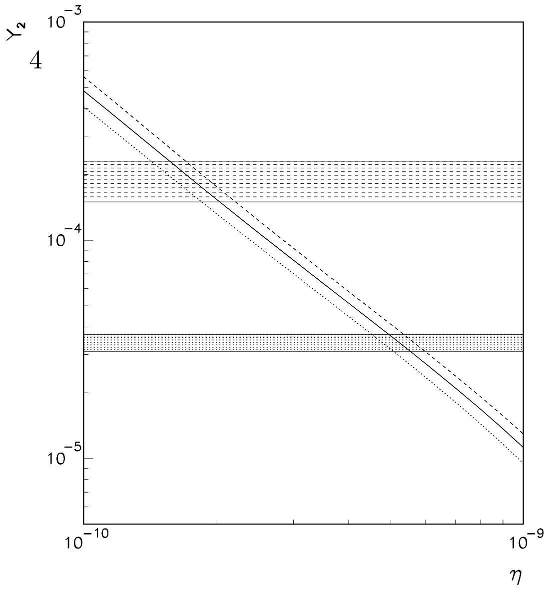

Figure 4. The quantity Y_2 versus η is reported. The same notation of Fig. 3 is used. The horizontal bands dashed and dotted are the experimental values (see for example [5]).

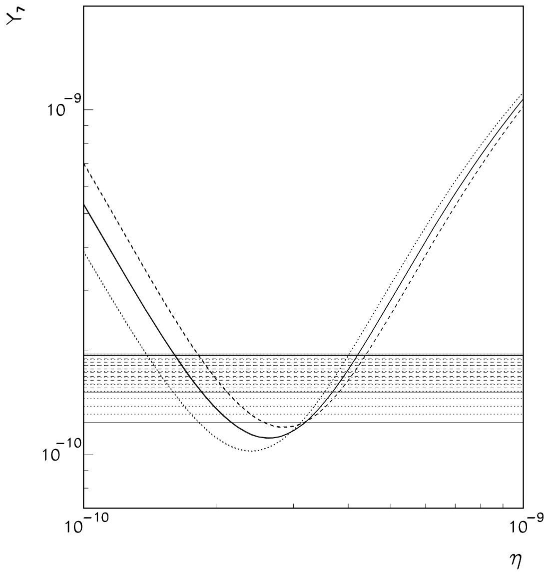

Figure 5. The quantity Y_7 versus η. The same notation of Fig. 3 is used. The horizontal bands dashed and dotted are the experimental values (see for example [5]).

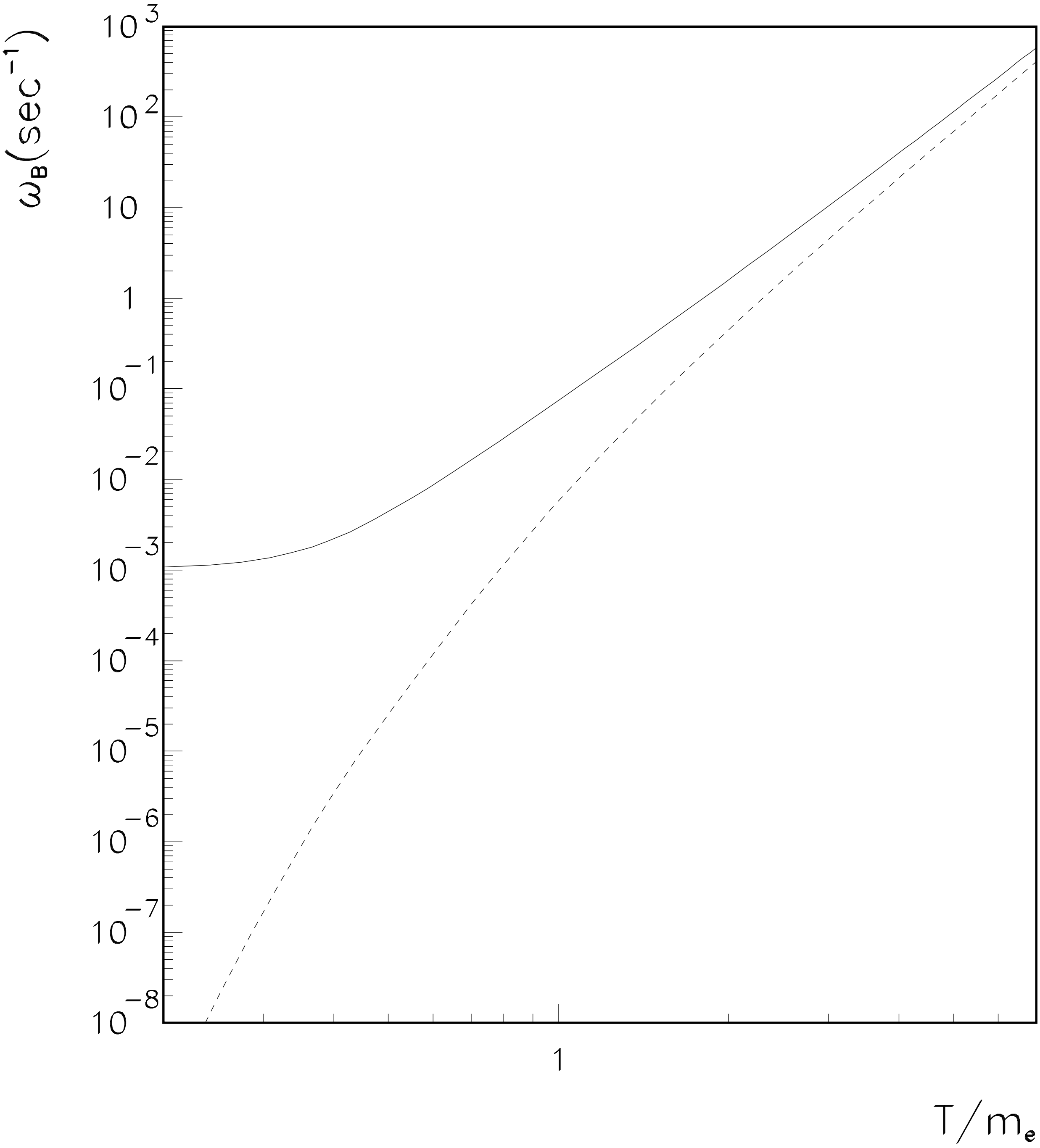
$\omega_B(\sec^{-1})$
10^3
10^2
10
1
10^{-1}
10^{-2}
10^{-3}
10^{-4}
10^{-5}
10^{-6}
10^{-7}
10^{-8}
1
T/m_e

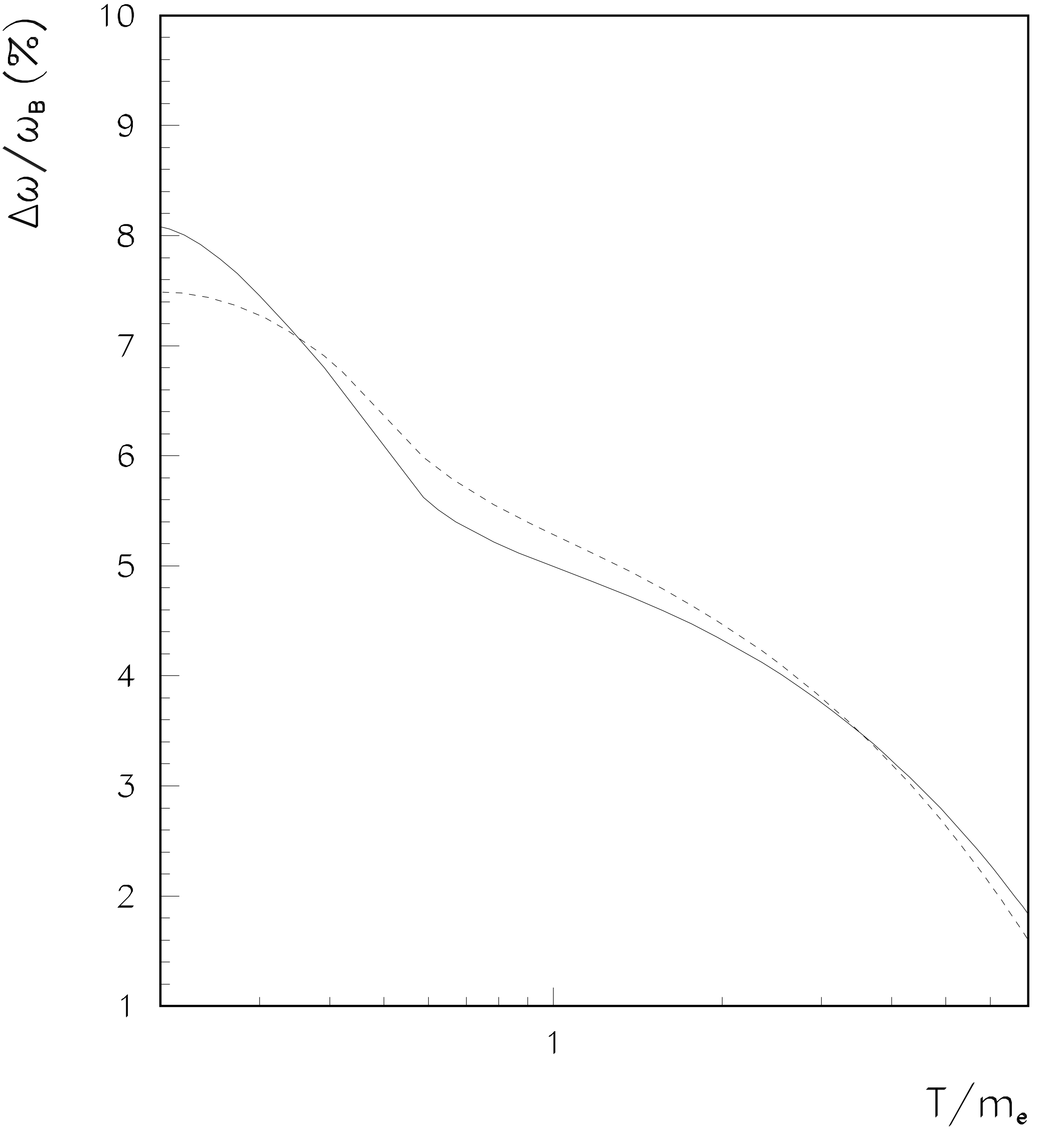

10
9
8
7
6
5
4
3
2
1
1
Δω/ω_B (%)
T/m_e

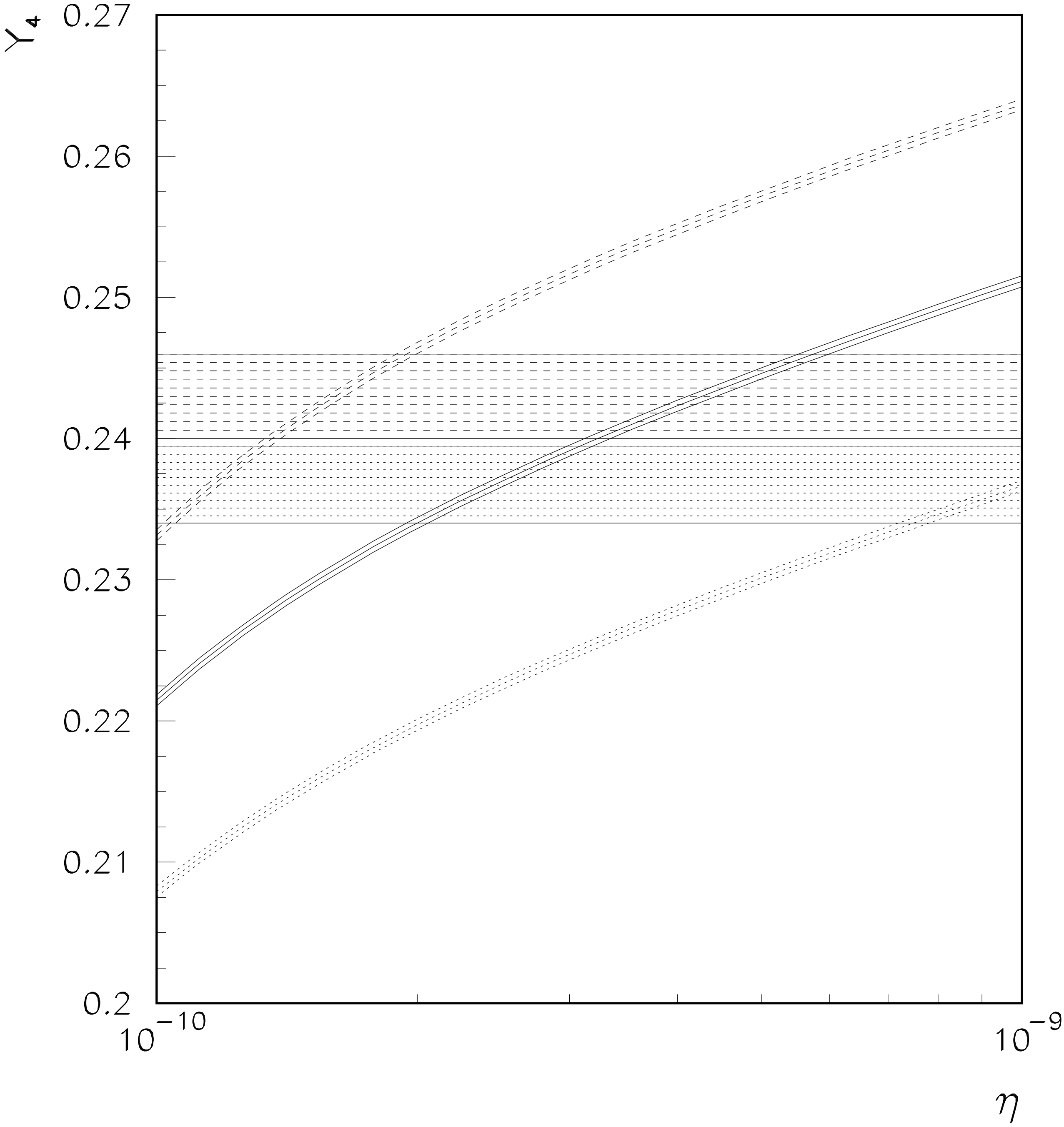

Y_4
0.27
0.26
0.25
0.24
0.23
0.22
0.21
0.2
10^{-10}
10^{-9}
η

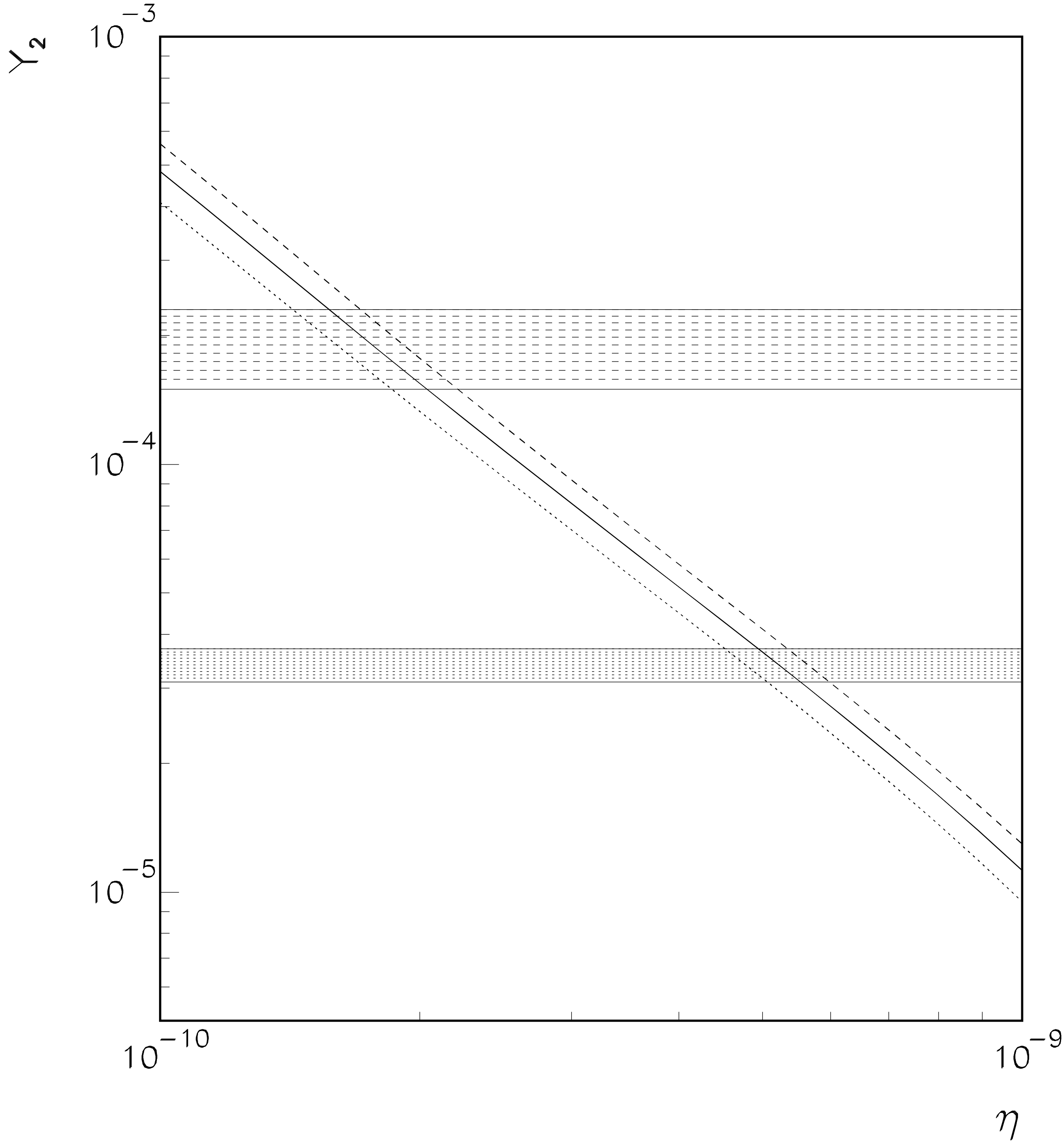

Y_2
10^{-3}
10^{-4}
10^{-5}
10^{-10}
10^{-9}
η

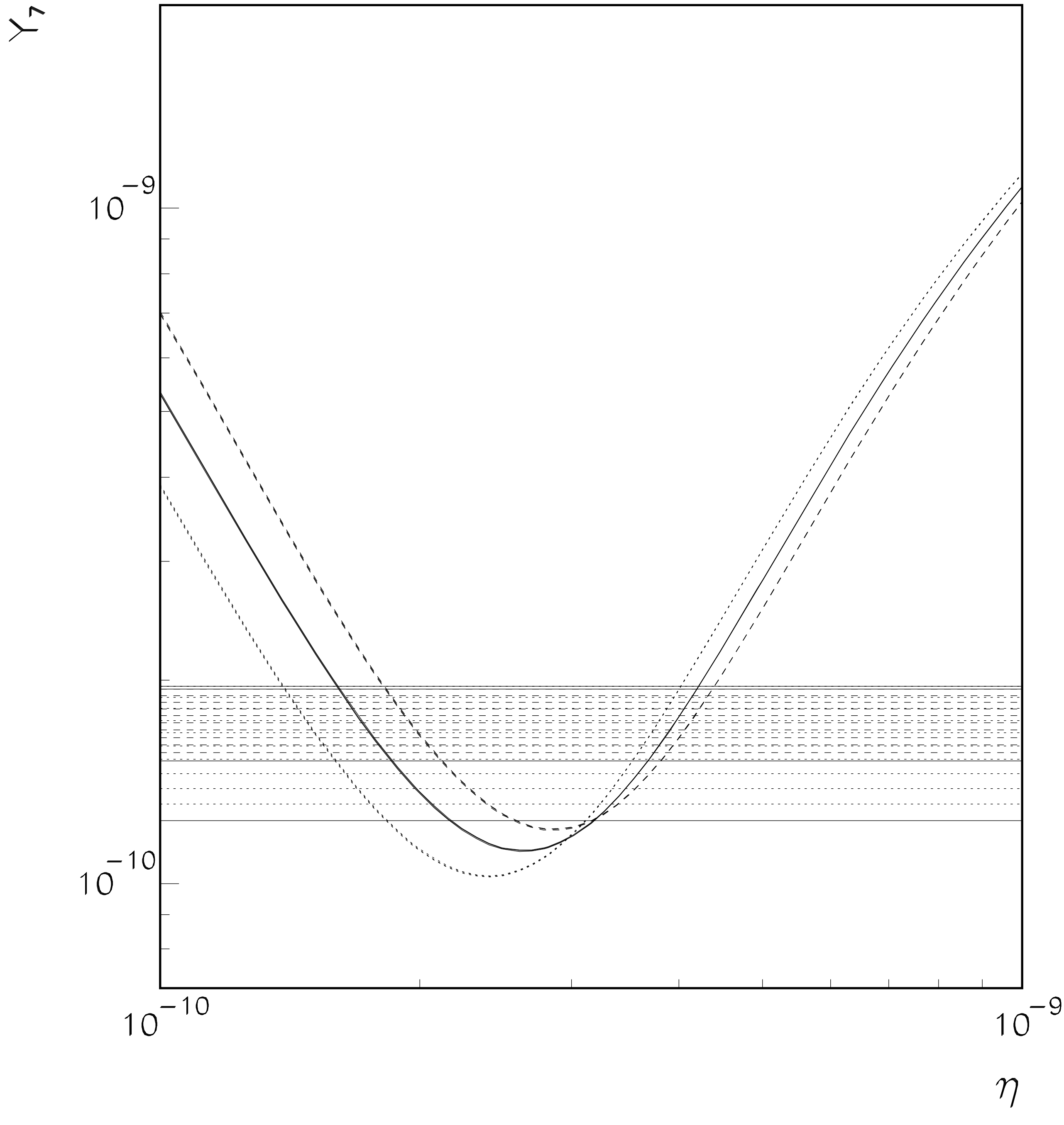
Y_7
10^{-9}
10^{-10}
10^{-10}
10^{-9}
η